



THE UNIVERSITY *of* EDINBURGH

Edinburgh Research Explorer

The World Trade Center 9/11 Disaster and Progressive Collapse of Tall Buildings

Citation for published version:

Kotsovinos, P & Usmani, A 2013, 'The World Trade Center 9/11 Disaster and Progressive Collapse of Tall Buildings' *Fire Technology*, vol 49, pp. 741-765., 10.1007/s10694-012-0283-8

Digital Object Identifier (DOI):

[10.1007/s10694-012-0283-8](https://doi.org/10.1007/s10694-012-0283-8)

Link:

[Link to publication record in Edinburgh Research Explorer](#)

Document Version:

Publisher final version (usually the publisher pdf)

Published In:

Fire Technology

General rights

Copyright for the publications made accessible via the Edinburgh Research Explorer is retained by the author(s) and / or other copyright owners and it is a condition of accessing these publications that users recognise and abide by the legal requirements associated with these rights.

Take down policy

The University of Edinburgh has made every reasonable effort to ensure that Edinburgh Research Explorer content complies with UK legislation. If you believe that the public display of this file breaches copyright please contact openaccess@ed.ac.uk providing details, and we will remove access to the work immediately and investigate your claim.





The World Trade Center 9/11 Disaster and Progressive Collapse of Tall Buildings

Panagiotis Kotsovinos and Asif Usmani, School of Engineering, The University of Edinburgh, Edinburgh EH9 3JF, UK*

Received: 4 December 2011/**Accepted:** 16 July 2012

Abstract. The collapse of the World Trade Center buildings on September 11, 2001 posed questions on the stability of tall buildings in fire. Understanding the collapse of the WTC Towers offers the opportunity to learn useful engineering lessons in order to improve the design of future tall buildings against fire induced collapse. This paper extends previous research on the modelling of the collapse of the WTC Towers on September 11, 2001 using a newly developed “structures in fire” simulation capability in the open source software framework OpenSees. The simulations carried out are validated by comparisons with previous work and against the findings from the NIST investigation, albeit not in the forensic sense. The column “pull in” that triggers the instability of the structure and leads to collapse is explained. The collapse mechanisms of generic composite tall buildings are also examined. This is achieved through carrying out a detailed parametric study varying the relative stiffness of the column and the floors. The two main mechanisms identified in previous research (weak and strong floor) are reproduced and criteria are established on their occurrence. The analyses performed revealed that the collapse mechanism type depended on the bending stiffness ratio and the number of floors subjected to fire and that the most probable type of failure is the strong floor collapse. The knowledge of these mechanisms is of practical use if stakeholders wish to extend the tenability of a tall building structure in a major fire.

Keywords: Structures in fire, Progressive collapse, Tall building collapse mechanisms, WTC collapses, Nonlinear dynamic thermo-mechanical analysis of structural frames, OpenSees

1. Introduction

The collapse of the World Trade Center buildings in a terrorist attack shocked the world because of the sheer magnitude of life loss and the grave implications of this event on the future of global peace and security. It also shocked structural engineers and architects as these were the first large modern steel frame buildings to collapse where fire could be described as the key contributing factor (impact damage did not cause collapse). Hence questions naturally arose on the stability of tall steel frame buildings in fire which needed to be addressed in order to properly explain and understand the cause of these collapses. These questions have assumed much greater urgency as the collapse of the WTC towers ironically coincided with the beginning of a decade of a tremendous surge in the building of

* Correspondence should be addressed to: Asif Usmani, E-mail: asif.usmani@ed.ac.uk

more and more super-tall buildings around the globe complemented by great innovation in the design of the super tall structures [1]. The engineers and architects seem to have shaken off their initial shock seeking comfort in the implausibility of the recurrence of a similar event and the security measures taken by the aviation industry [2]. The role that the fire had on these events, and thus the potential impact on other super-tall buildings, has thus been relegated to a lower level of importance [1].

Forensic investigation on the collapse of WTC towers was performed by the Federal Emergency Management Agency [3] and subsequently more comprehensively by the National Institute for Standards and Technology [4]. A summary of the structural design of the WTC complex and NIST's findings can also be found in the current special issue [5–8]. Other smaller scale independent research studies were carried out by Quintiere et al. [9], Usmani et al. [10], Kodur [11], Usmani [12] and Flint et al. [13]. The FEMA report and Quintiere et al. studied the large deflections that were developed in the composite floor during the fire but did not present a clearly defined collapse mechanism. Usmani et al. and the NIST report identified that the instability that triggered the collapse was not from the aircraft damage or connection failure but from the interactions between the fire and the structure. NIST focused on reproducing the specific sequence of events and attempted to carry out a coupled analysis as far as possible, as advocated recently by Baum [14]. In contrast to this, Usmani et al. concentrated on the vulnerabilities of the particular structural form, not including the aircraft damage but concentrating on the fire-structure interactions for a large range of parameterised temperature evolutions, in terms of growth rate, magnitude and spread. In both sets of studies a consistent global collapse mechanism where the perimeter columns were pulled in was found. NIST demonstrated that this sequence of events was in accordance with the photographic evidence.

The effect of perimeter columns in the structural behaviour in fire has been investigated in the past both experimentally and computationally. Ali and O'Connor [15] investigated experimentally the structural fire performance of columns under different rotational constraints. Franssen [16] compared the effect of the interaction of a column as part of a frame and as a single element. He used the arc length procedure in order to follow the postbuckling response of columns in fire. Huang et al. [17] examined numerically the internal forces, stresses and strains developed in columns under axial and moment loads and a uniform temperature profile. Results indicated that moments become important when the columns are not rotationally restrained. Shepherd and Burgess [18] also investigated the buckling and postbuckling behaviour of columns in fire including the snap through and snap back phases. They pointed out that robustness is essential in order for load redistribution to take place and for avoiding progressive collapse. Previous research conducted by Quiel and Garlock [19] compared the performance between 2D plane and 3D analysis for high rise buildings under fire. Their results indicated that a 2D plane analysis can adequately predict the interaction between the perimeter column and the floor slab.

This study expands further the concepts that were presented by Usmani et al. [10] based on the same assumptions. The parametric treatment of fire, representing

it as predefined temperature versus time curves, is akin to a design approach and not a forensic treatment. Therefore, this study does not address the time to failure or any pre-existing damage and focuses on understanding the failure mechanism. This allows the study of the particular structural form to be free from forensic aspects [20] and with a defined objective of understanding the behaviour of these structures to derive lessons that will improve future designs. This study will also examine further the two generic collapse mechanisms (the *strong floor* and the *weak floor* mechanisms) for tall buildings in the event of fire based on previous work by Usmani et al. [21] in order to draw useful lessons from this major structural engineering failure.

2. Model

2.1. Structural Layout

The two towers of the WTC encompassing 110 stories above ground were almost identical. They were built using a unique structural system exploiting the tube concept of Dr Fazlur Khan [22] to resist the immense wind loads on very tall buildings, coupled with an ultra-light truss floor system, all optimised for rapid construction. The details of the structural system including splices and connections and individual member dimensions are available in the publications by FEMA [3] and NIST [4].

The model presented in this paper is identical to the one used in Usmani et al. [10], however a completely different software (OpenSees, [23]) is used. A two-dimensional sub-structure representing a 12 storey slice of the tower along the longest span floor area is modelled, assuming the core to be rigid. More specifically floors 90–101 are represented in the model. The typical dimensions of structural members included in the model are shown in Figure 1 (FEMA [3]). As shown in the figure, the composite truss floor system is assumed to be rigidly restrained against translation against the rigid core but is free to rotate (thus a pinned connection was used at the right end). The column to floor connection is also a pinned connection, constraining the translation degrees of freedom of the floor nodes to be equal to those of the column nodes but keep rotations independent.

The actual composite floors had a span of 60 ft (~ 18.29 m) (in the longer span direction) with a concrete deck thickness of 4 inches (~ 101 mm) and a truss depth of 29 inches (~ 737 mm). The truss' top and bottom chords were made from back to back angles of an equivalent area of 1.5×1.5 inches ($\sim 38 \times 38$ mm) and the diagonals had a diameter of 1.09 inches (~ 28 mm). The storey height was 12 ft (3.6 m) and the columns were 350 mm square hollow sections with varying plate thickness along the height of the column, which at the height considered here was 6 mm. The truss' diagonals had a spacing of 40 inches (1.016 m) generally through the span, with the end diagonals being 13.33 ft (2.032 m) long. The composite floor was modelled using a span of 18 m, with diagonals spaced at 1 m and the end diagonal was assumed to be 2 m long. The truss was assumed to have a depth of 740 mm.

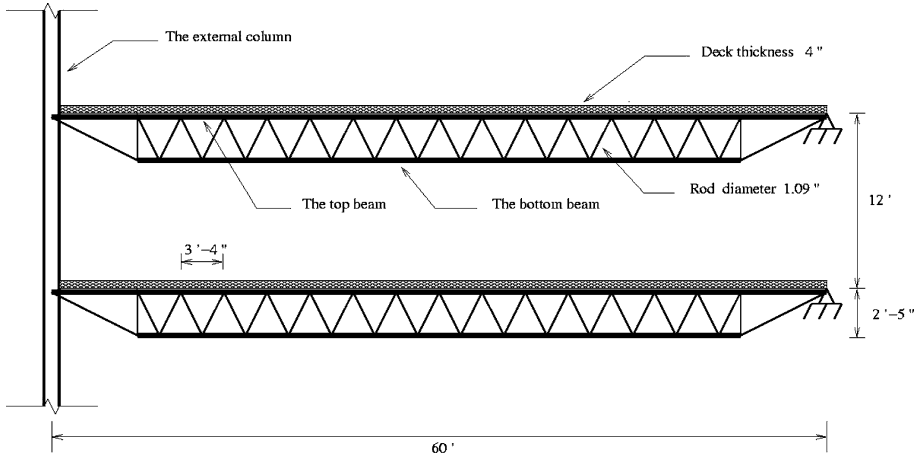


Figure 1. WTC towers typical structural layout.

2.2. Finite Element Modelling

2.2.1. OpenSeeS. The current finite element model (Figure 2) was constructed using the open-source and object-oriented structural engineering software framework OpenSees [19, 20]. OpenSees is effectively a library of advanced computational tools for the nonlinear analysis of structures. The OpenSees framework is being extended at the University of Edinburgh by adding classes that introduce into OpenSees the capability of performing analyses of structures in fire including both heat transfer and thermo-mechanical analysis [25]. This work aims to enable the analyst to perform state of the art nonlinear analysis of structures under different situations (fire or earthquake) or multi-hazard (fire after earthquake) in a single numerical tool. The work so far includes truss and two dimensional beam column elements with temperature dependent nonlinear uniaxial materials based on the thermo-mechanical properties for steel and concrete published in the Eurocodes (EN1992 and EN1993). Three-dimensional elements are also being developed and tested.

OpenSees was chosen to carry out these studies so that the results from the newly developed code could be compared to previous research carried out with ABAQUS and hence help validate the code developments. Once all the new developments are validated and tested on a number of different operating systems, they will be offered to be included in a future general release of OpenSees (by PEER and UC Berkeley) so that any interested engineer or researcher can examine and criticise this work and use the software freely for research purposes.

2.2.2. Meshing. All the structural members (columns, slab and truss) were modelled using the two-dimensional two-node *dispBeamColumn2DThermal* elements. These elements are modified versions of the original *dispBeamColumn2D* elements available in OpenSees that account for fire induced internal forces. *DispBeamColumn2D*

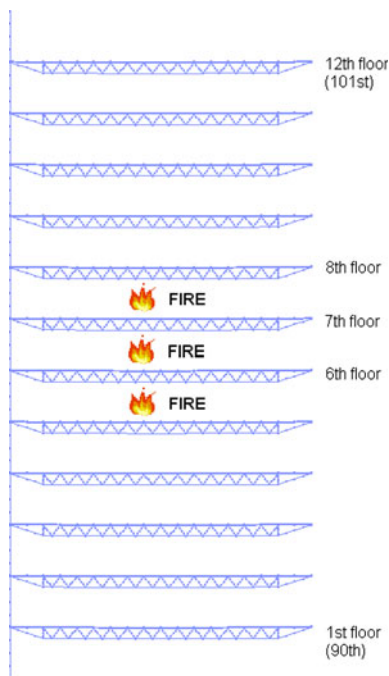


Figure 2. OpenSeeS finite element model of the WTC Tower.

elements are formulated using the finite element method and adopt a distributed (or spread of) plasticity concept which requires the user to select a number of integration points (or control sections) [26–28]. Five integration points were used for this study. Each control section usually represents a pre determined *fiberSection*. According to the *fiberSection* approach a cross-section is discretized (e.g., unilateral discretization, radial discretization) into a number of fibers where each fiber has a prescribed uniaxial stress–strain relationship. The nonlinear geometry under large displacements (for example, as present in beams during a fire) can be incorporated by using a co-rotational formulation which transforms the coordinates to the global system. A sufficient number of these elements must be used in order to capture the nonlinear behaviour of the members (including p-delta type effects caused by restrained thermal expansion). At least four elements were used for each truss diagonal, bottom chord and top chord. This allowed the model to adequately capture the buckling of the compression diagonals and other members susceptible to buckling under heating induced restrained thermal expansion.

A uniform load of 5 kN/m was applied to the floors. This value corresponds to the permanent and variable loads of the structure and was taken from NIST report [4]. Columns were subjected to a point load of 360 kN representing the load coming from storeys above. This value was calculated taking into account 40% of the load coming from the uniform load (permanent and variable) acting on the nine floors above this twelve storey model.

2.2.3. Composite Action. The composite slab is modelled using separate beam-column elements for the top chord and the slab. In order to model the composite action between the concrete slab and the top chord of the steel truss, *rigidLink* constraints were used for the corresponding translations and rotation of the nodes. *rigidLink* is a multi freedom constraint which ties the degrees of freedom of a slave node to follow that of a master node. In this model the case of bond slip is not taken into account and the slab is assumed to act in full composite action with the top chord for the whole duration of the analysis. Therefore failure of shear connectors cannot be modelled [29]. Shear connector failures typically begin at the ends of the composite member and therefore may not have a significant global impact however this issue is not addressed in this paper.

2.3. Materials

Several fire resistance tests of structural members have shown that high temperature causes material degradation so the reduction of material properties like Young's modulus and Yield Stress have to be accounted for by utilizing appropriate constitutive relationships. Hence, new uniaxial elastic plastic material models have been developed by modifying appropriately the existing ones under the OpenSees framework that take into account the material degradation under elevated temperatures, the steel bilinear material model (*Steel01Thermal*), the steel elliptic material model (*Steel02Thermal*), and concrete material model (*Concrete02Thermal*).

The material properties are not exactly known and varied along the height of the structure so typical properties were used. For the steel members (column, truss members) a yield strength of 300 N/mm² and modulus of elasticity of 210 GPa were assumed. The concrete slab was assumed to have a compressive strength of 30 N/mm² and a tensile strength of 5% of its compressive strength. The steel reinforcement was assumed to have yield strength of 475 N/mm².

2.3.1. Numerical Algorithm. Quasi-static integration methods like load control have significant limitations in dealing with local or global instabilities that commonly occur in modelling structures subjected to fire (because of the stresses generated by restraining thermal deformations). For this reason an implicit dynamic procedure has been used in this work to trace post-buckling response of members and overcome instability points. The numerical scheme selected for the dynamic analysis is an implicit solution with a Hilber–Hughes–Taylor integrator with $\alpha = 0.7$ to add numerical damping to the model [30].

2.4. Fire Input

Due to the aircraft impact on the structure and the fuel that caused ignition on the furniture, it can be assumed that multiple floor fires were developed at the same time in the tower [11]. For this work the fire is assumed to be simultaneous and on floors 5, 6 and 7 of the finite element model.

A generalised exponential curve is chosen to represent the time–temperature relationship and is given by Equation (1)

$$T(t) = T_0 + (T_{\max} - T_0)(1 - e^{-at}) \tag{1}$$

where T_{\max} is the maximum temperature (800°C in this study), T_0 is the ambient temperature (20°C), a is a rate of heating parameter (0.005) and t is the time (3,600 s).

This fire curve is very general and it is not argued that it represents the fire that was seen in the case of the WTC towers; nevertheless, the range of temperatures covered is consistent with the fire modelling conducted by NIST [4]. As this paper is examining the collapse mechanism and not trying to reproduce the failure time, a parametric approach to the fire is reasonable.

Since the fire occurs on floors 5–7 (corresponding to floors 94–96 of the towers), the members affected are the composite trusses on floors 6–8 and the columns supporting them. Steel sections are assumed to be heated uniformly in contrast to concrete sections where thermal gradients appear. The columns are assumed to be protected and hence heated to a maximum temperature of 400°C while the steel truss is assumed to be unprotected and at the same temperature with the fire, being heated to a maximum temperature of 800°C. For the temperature distribution in the concrete slab, a 1D heat transfer analysis was performed. These time temperature curves can be seen in Figure 3.

Due to the fact that the interface between the thermo-mechanical analysis part of OpenSees and the heat transfer part is still under development, the temperature evolution in the structural members from the fire was assigned manually.

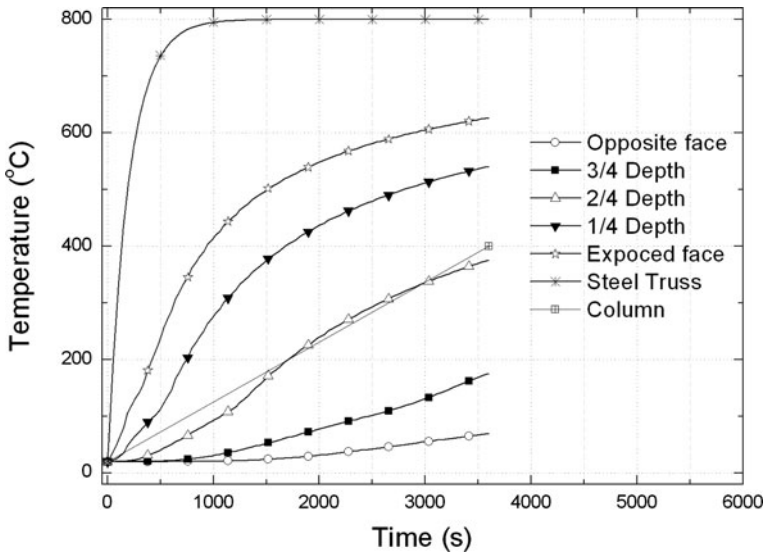


Figure 3. Temperature distribution of the structural members.

3. Analysis and Results

3.1. Description of Global Behaviour

The global behaviour of the structure can be seen from Figure 4 showing the deformed shape of the model. It can be seen that collapse occurs with the columns being pulled inside because of the large deflections in the floor. The horizontal displacement of the columns of the fire-affected floors is plotted in Figure 5. At an early stage of the fire the composite floors expand and the column is pushed outward by approximately 50 mm at about 150 s which corresponds to a fire temperature of 430°C. After this point the column is suddenly pulled in but stabilises and continues to displace inwards until the structure becomes irreversibly unstable at 250 s (fire temperature of 580°C). It is also of interest to note that when collapse occurs the column is almost at ambient temperature. Figure 6 illustrates the vertical displacement of the columns for floors 5–9 also showing collapse at 250 s.

Horizontal reactions at the floor connection to the stiff core show the change in membrane forces over temperature. Figure 7 illustrates that the middle fire floor is in tension initially but snaps into compression before failure occurs and then goes into tension again at the initiation of collapse. The top and bottom fire floors along with floors 4 and 10 experience compression until initiation of failure when they snap into tension. In contrast floors 5 and 9 are in tension and snap into compression at this point.

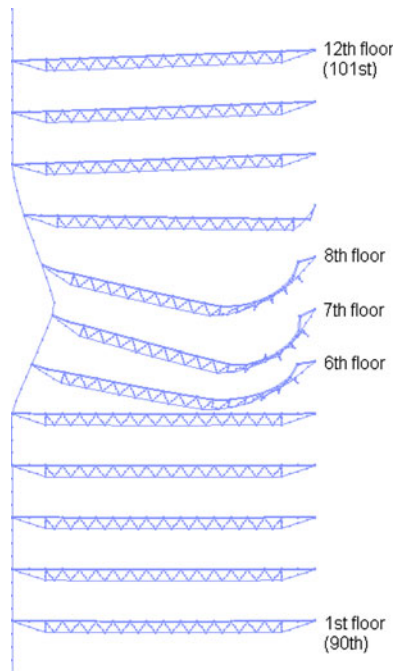


Figure 4. Deformed shape of the WTC Tower model.

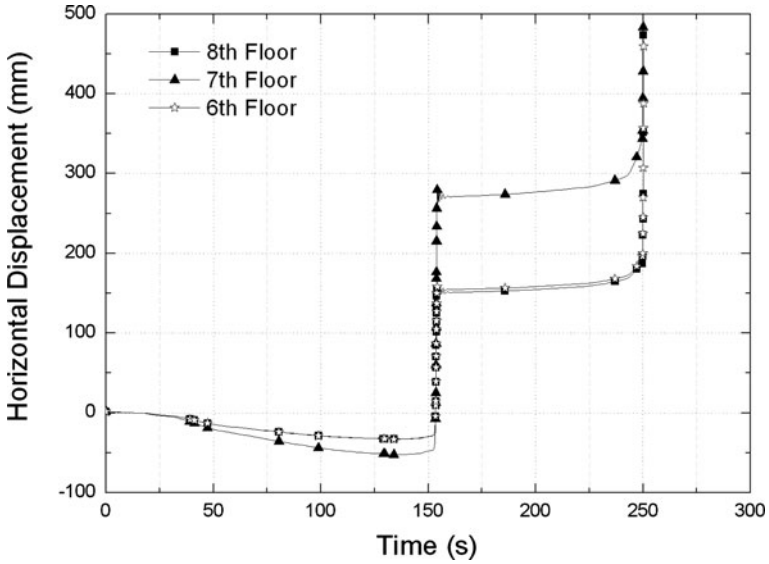


Figure 5. Horizontal displacements of floor-column joint nodes.

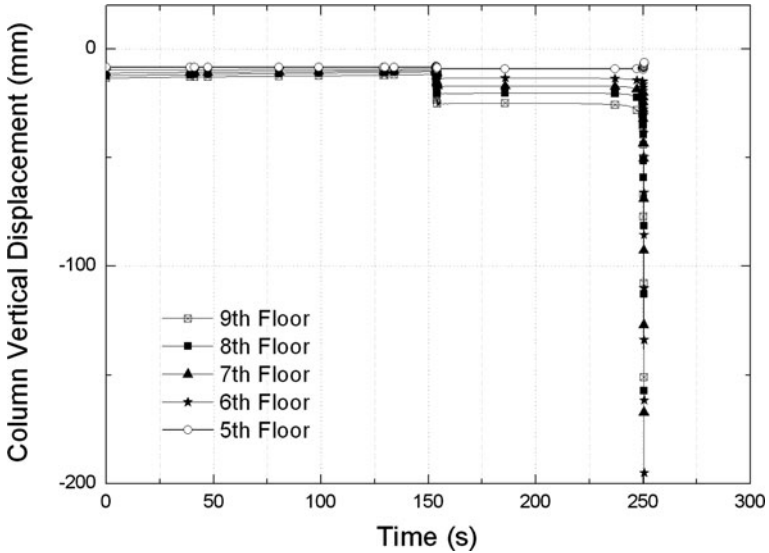


Figure 6. Vertical displacement of floor-column joint nodes.

Figure 8 plots the section moments in the column at the floor-column joint node. It can be seen that at around 150 s section plastic moment capacity is reached which initiates strong floor collapse. Figure 9 shows the column plastic rotation for floors 5, 7 and 9. The calculation of plastic rotation in OpenSees is performed by deducting the yield or recoverable rotation by the maximum

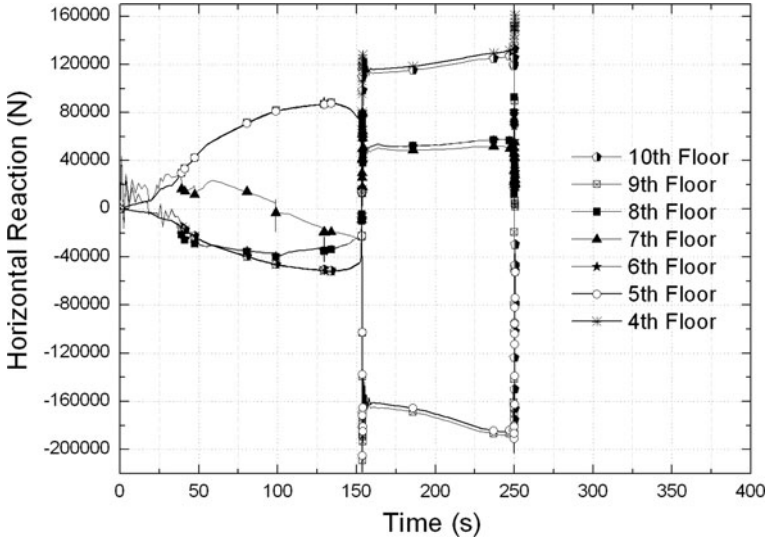


Figure 7. Membrane forces in the floors.

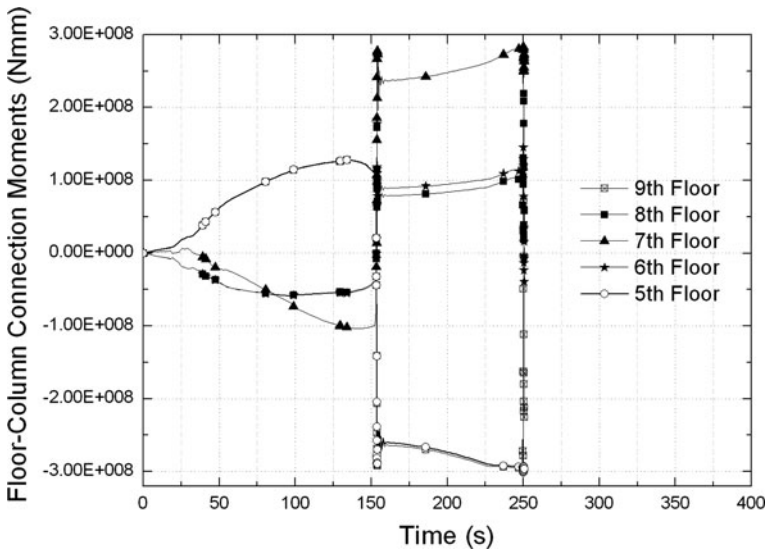


Figure 8. Column section moments at floor-column joint nodes.

absolute total rotation. This graph clearly shows that a plastic hinge mechanism has been formed.

3.2. Behaviour of the Truss System

In Figure 10 the plot of midspan deflection of the floors versus time is shown indicating the same pattern of behaviour as in the previous two figures. The large

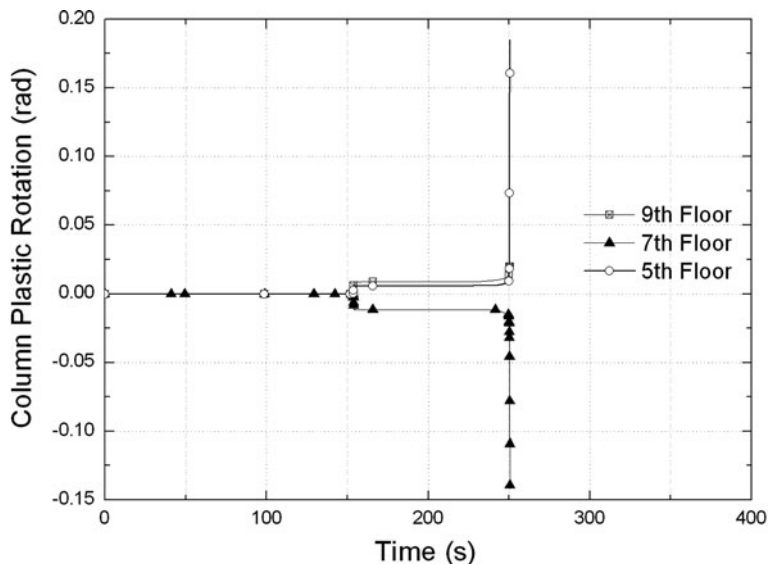


Figure 9. Column plastic rotations at floor-column joint nodes.

displacements, internal forces and material degradation cause the truss diagonals to buckle, particularly members located near the support to the stiff core. These members experience relatively larger forces arising from the restrained thermal expansion of the floor.

The axial forces in some critical members of the top chord at the 7th floor are shown in Figure 11 where members are numbered from the left to the right (so member 2 is near the column and member 15 is near the rigid core). The top chord is in compression as the temperature increases until the first instability at 150 s and remains in compression for most its length during collapse. In contrast Figure 12 indicates that all the bottom chord members (numbered from left to right) were in tension for the whole duration of the fire until collapse but initiation and ultimate collapse are still indicated by sudden changes in magnitude. Figure 13 also displays axial forces in the inner truss diagonals (numbered from left to right) including the right end inclined and vertical members for the 7th floor of the model. The highest loaded compression diagonals are as expected the outer most compression diagonals (2nd and the 27th). As in the other figures the initiation and ultimate collapse are reflected in internal load redistributions in Figure 13 as well.

4. Parametric Study on the Collapse Mechanisms of Tall Buildings in Fire

Previous research by Usmani et al. [21] has investigated the behaviour of tall buildings in fire with similar structural form to the WTC towers but with more

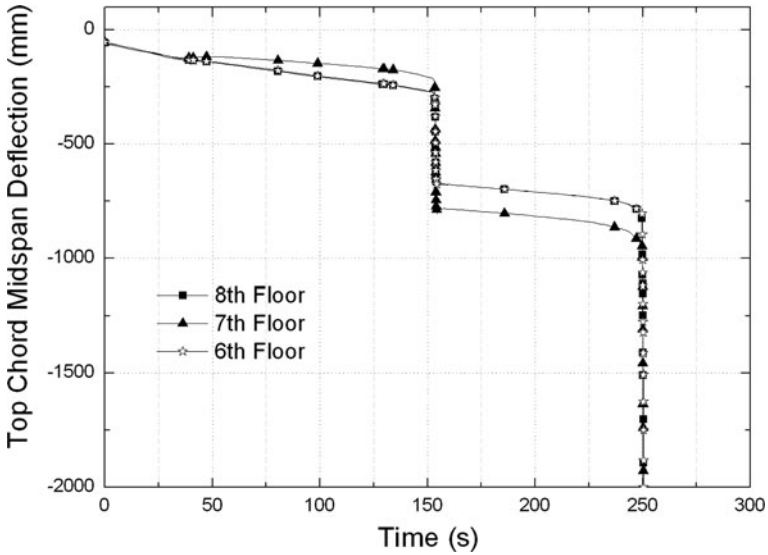


Figure 10. Midspan deflection of the floors.

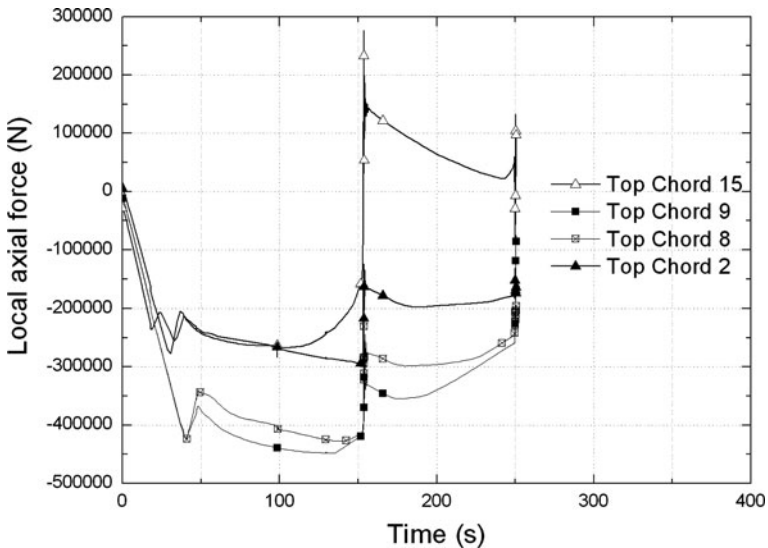


Figure 11. Top Chord axial forces for the 7th floor.

generic sections for columns and beams instead of tubular columns and trusses. Their research has shown that the same collapse mechanisms are possible. Furthermore, two distinctive collapse mechanisms can be identified, namely the ‘weak floor’ and ‘strong floor’ mechanisms. The analysis presented here will reproduce these mechanisms and establish criteria that lead to one or the other based on a

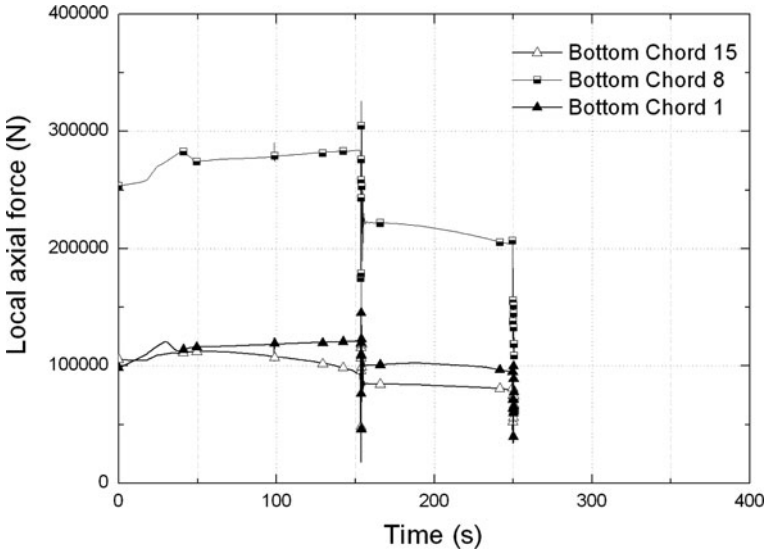


Figure 12. Bottom Chord axial forces for the 7th floor.

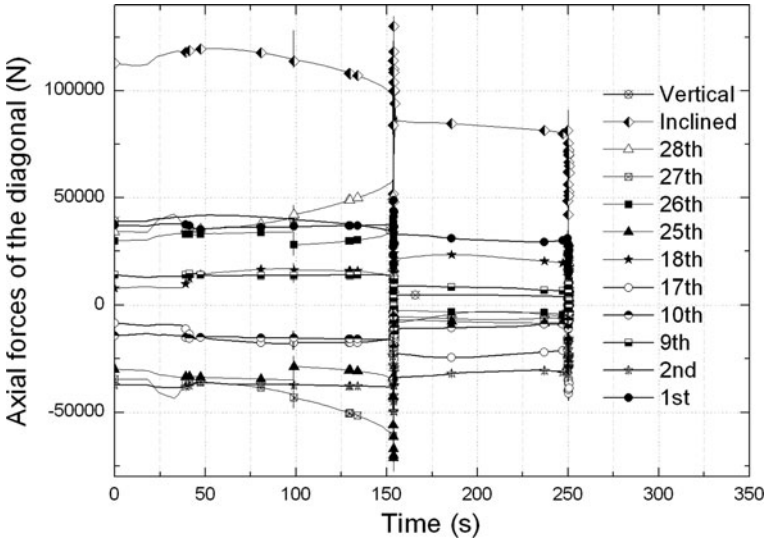


Figure 13. Axial forces in the diagonals for the 7th floor.

parametric study. For the analyses performed in this paper the building will be assumed to have a fixed beam-column connection at the column end. This assumption, unlike in the WTC Towers shown previously, implies that both translation and rotation of the beam and column nodes are constrained to be the same. But as for the WTC Towers model the possibility of connection failure is not

taken into account. At the rigid core end the steel beam and the slab (forming the composite floor) are both pinned to a rigid lateral restraint. This connection also simulates a fixed-end connection for the composite floor.

4.1. Weak Floor and Strong Floor Failure Mechanisms

The structural model used is similar to the one used earlier except for universal beam and concrete slab composite floors and universal columns (instead of tubular columns and composite truss floors).

Previous research identified the two distinctive mechanisms but clear criteria governing the collapse mechanism type were not established. These criteria are based on the behaviour of the “bottom pivot” floor (the floor immediately below the lowest fire floor), which in this paper is the 5th floor. If the bottom pivot floor reaches its plastic moment capacity at midspan (from $P-\delta$ moments induced because of having to provide a reaction to the “pull in” forces at the fire floors, see Figure 14a), a hinge is formed (see Figure 14a) in the floor and the weak floor mechanism is initiated. The bending failure spreads to the lower adjacent floor and then further downwards (with potentially a similar failure spreading upwards from the top pivot floor) leading to a progressive disproportionate collapse of the structure. If the bottom pivot floor is able to sustain the increasing bending moments, the column connecting the pivot floor may reach its plastic moment capacity first (as indicated by the hinge shown in Figure 14b) at a section near the floor-column connection which then initiates the strong floor failure. A three hinge mechanism forms with two further hinges in upper floors. The key distinction between the two collapse mechanisms is the initiation. In the weak floor mechanism collapse initiates due to bending failure of the bottom pivot floor itself, while in the strong floor mechanism collapse initiates due to combined compression and bending failure of the column adjacent to the bottom pivot floor. Figure 14 shows deformed shapes for weak and strong floor collapse under a three floor fire scenario (fire affected floors are floors 6–8).

4.1.1. Strong Floor Collapse. Figure 14 illustrates the two mechanisms as described above for a three floor fire in a model of a typical tall steel frame composite structure as described above. Figure 15 shows the horizontal displacements of the column at the level of the fire floors (with negative direction denoting outward movement and positive denoting inward movement). Figure 16 shows the midspan deflections at the fire floors and Figure 17 the horizontal reaction force at the rigid end restraints at the right. These reactions represent the membrane forces in the floors. It can be seen that initially the bottom and top fire floors and floors 4 and 10 are in compression (negative sign) and then snap into tension (positive sign) when failure initiates. On the other hand, the pivot floors, 5 and 9 are in tension and when failure begins they snap into compression. Floor 7 is in tension when the floors are expanding but then goes into compression when the pull in process starts and finally goes into tension again when failure occurs. Figure 18 shows the moments in the column at the level of the fire and pivot floors.

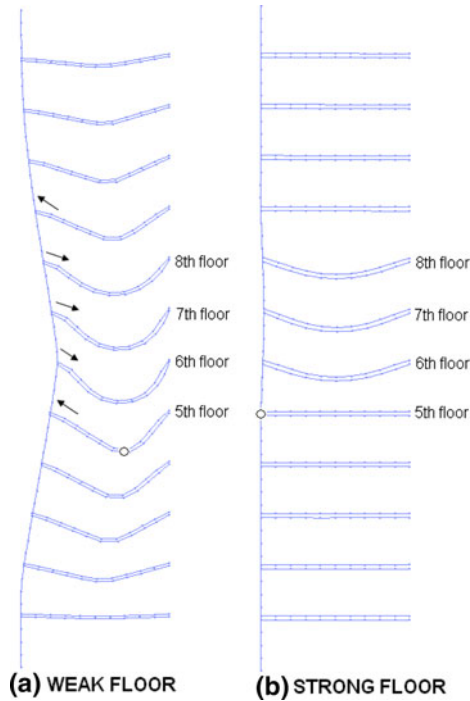


Figure 14. Deformed shapes of weak floor and strong floor failures.

The figure clearly shows the changes in column moments during outward displacement and the reversal of signs at the beginning of collapse as expected.

4.1.2. Weak Floor Collapse. Weak floor collapse, if possible, will occur at an earlier time for the same column than the strong floor collapse. This is initiated at the bottom pivot floor if it cannot sustain the additional moment demand from the $P-\delta$ moments induced by the “pull in” forces at the fire floors. Furthermore, weak floors expand much less than strong floors before the “pull in” phase starts (as shown in Figure 19). Figure 20 shows the vertical displacements of the column at the level of the fire floors, clearly indicating collapse.

Figure 21 clearly shows that the bottom and top pivot floors suddenly experience significant deflections after the fire floor deflections reach between 700 mm and 800 mm, which is indicative of bending failure in the pivot floors.

It can be seen in Figure 21 that the 5th floor (or the bottom pivot floor) of the structure also deflects when the collapse occurs. This indicates bending failure of the bottom pivot floor which does not occur in strong floor collapse and hence is a main distinguishing characteristic of weak floor collapse.

Figure 22 shows the variation of membrane forces at the connection of the floors to the stiff core. Here the behaviour is similar to the strong floor mechanism. It can be seen that initially floors 4, 6, 8 and 10 are in compression and

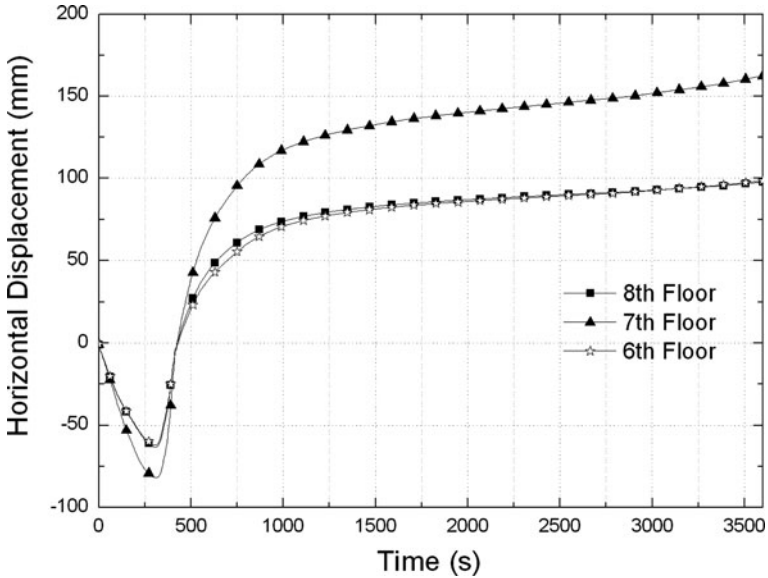


Figure 15. Horizontal displacement for the strong floor failure.

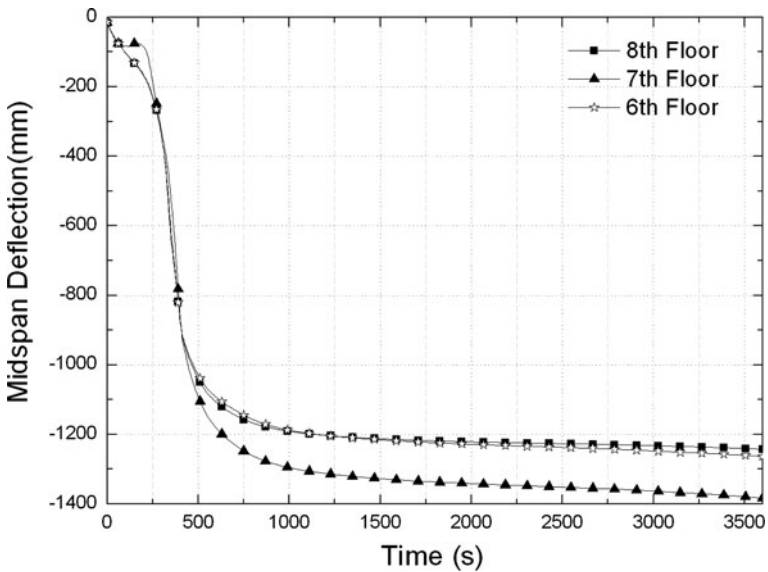


Figure 16. Midspan deflection for the strong floor failure.

later snap into tension while floors 5, 7 and 9 are initially in tension and then snap into compression. Figure 23 plots the variation of moments in the column. Similar changes occur during the pulling-in process like for the strong floor collapse.

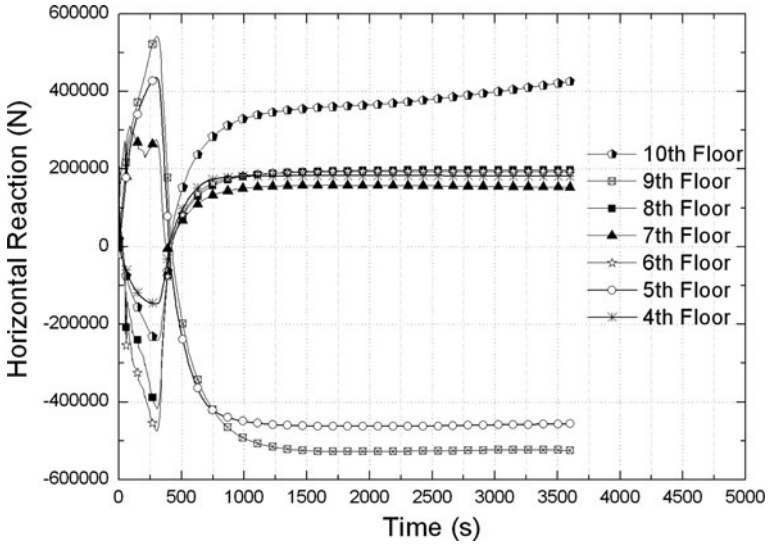


Figure 17. Horizontal reaction for the strong floor failure.

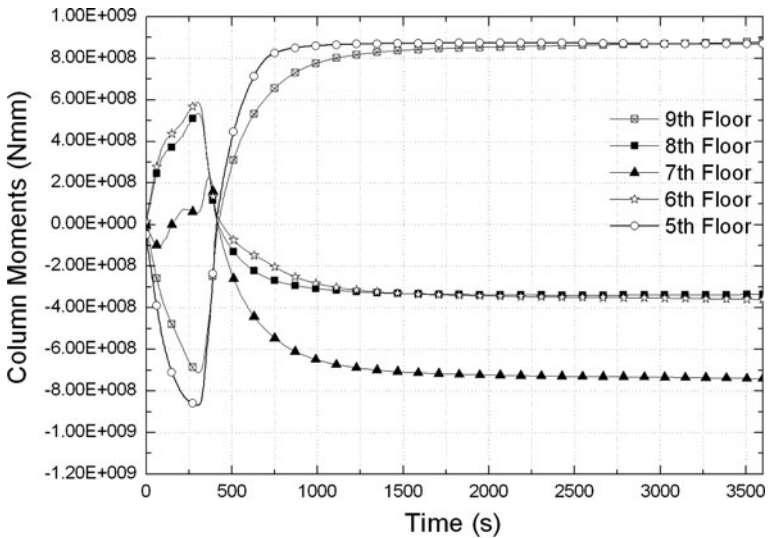


Figure 18. Column moments for the strong floor failure.

4.2. The Effect of Bending Stiffness of the Structural Members and Number of Floors in Fire

The analyses performed previously have identified that both types of collapse mechanisms are in bending, either in the floors or in the column. It could therefore be illuminating to examine the effect of different floor and column bending

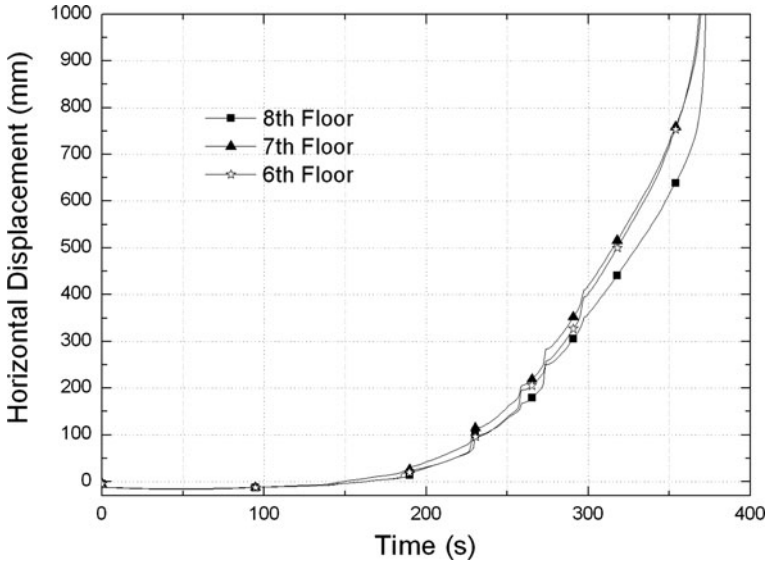


Figure 19. Horizontal displacement for the weak floor failure.

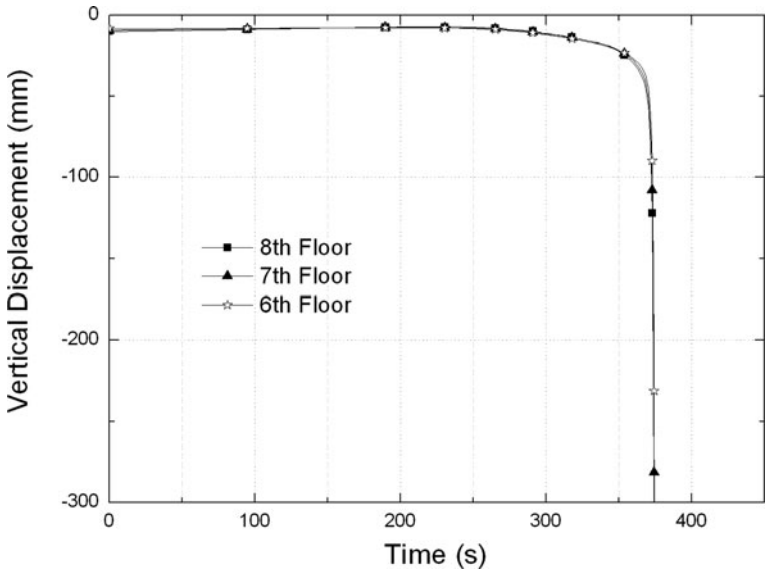


Figure 20. Vertical displacement for the weak floor failure.

stiffness combinations. It is also clear that the number of floors on fire will also be a significant factor in what type of failure mechanism occurs. When a greater number of floors are subjected to fire, the bottom pivot floor will need to carry greater moments because of the larger forces required to anchor the sagging fire floors in tensile membrane action.

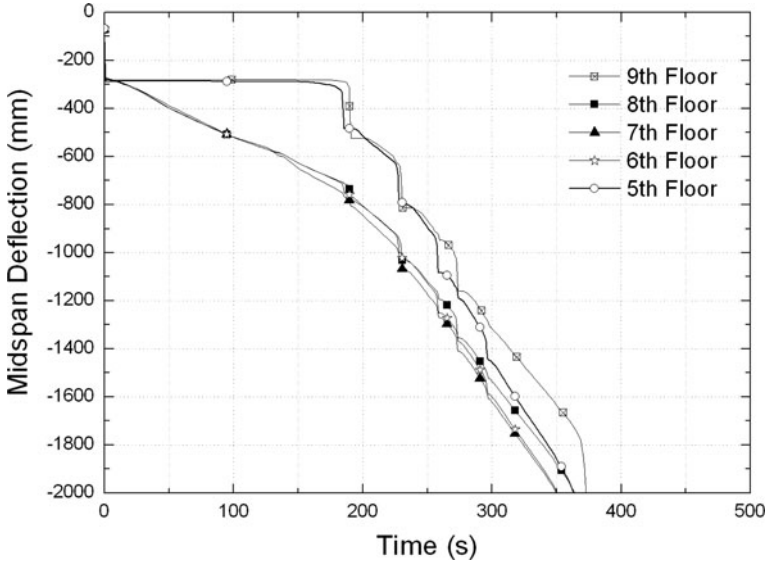


Figure 21. Midspan deflection for the weak floor failure.

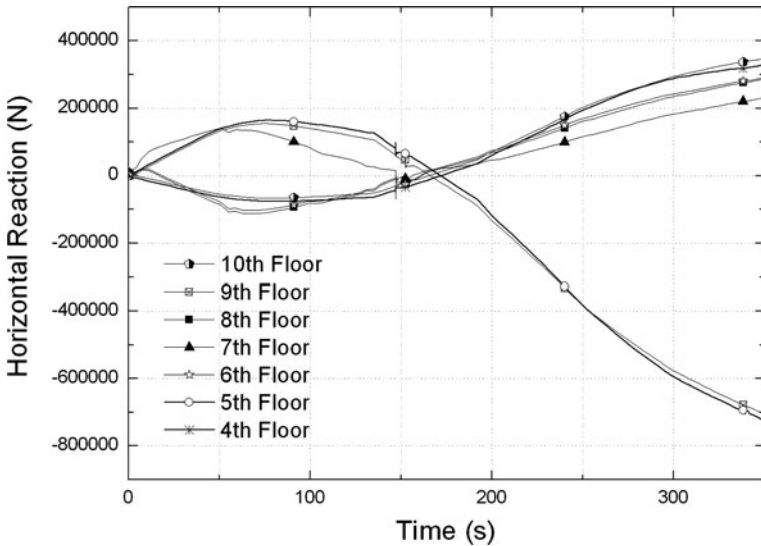


Figure 22. Horizontal reaction for the weak floor failure.

In order to investigate the effect of the ratio of bending stiffness between the column and floors, a number of analyses were performed keeping constant the height of the column (4 m), the length of the floor (10 m) and the concrete slab depth (100 mm) and its width (6 m) but varying the steel sections.

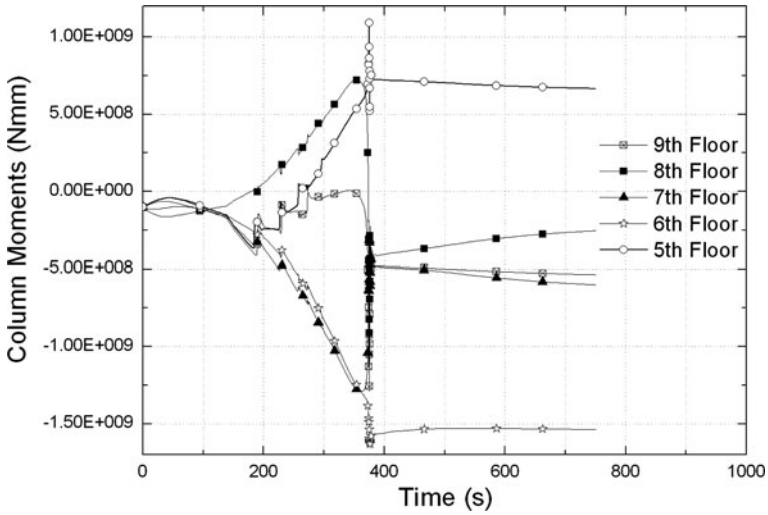


Figure 23. Column moments for the weak floor failure.

The ratio is defined as,

$$\frac{S_{column}}{S_{floor}} = \frac{(E_C I_C / L_C)}{(E_F I_F / L_F)}$$

These quantities are calculated using the transformed area method for the floors as they are composite members. A wide range of different scenarios were considered for this paper. An indicative illustration is shown in Table 1.

Figure 24 shows deformed shapes for weak and strong floor collapse under a four floor fire scenario (fire floors are 6–9) and Figure 25 shows deformed shapes for weak and strong floor collapse under a five floor fire scenario (fire floors are 6–10). These figures also denote where the first plastic hinge is formed in the pivot floor or in the pivot floor-column joint node for the weak floor and strong floor collapses. The 5th floor is always the bottom pivot floor in this paper.

The analyses performed revealed that the collapse mechanism type depended on the bending stiffness ratio and the number of floors subjected to fire, as illustrated in Figure 26. The hatched area in the figure shows a fuzzy region where either type of failure can occur. This sort of a diagram would allow a very quick check to determine what sort of failure could be expected for a particular building under multiple floor fires keeping in mind that the possibility of failure of connections or shear connectors is not taken into account. This is useful information in case a weak floor collapse is indicated. Strengthening of the floors and conversion to a strong floor collapse would considerably extend the tenability of the structure and hence the time available for egress and intervention. In earthquake engineering strong columns and weak beams are preferred which seems to contradict the recommendation given here. This however is non-issue, because for strong floor collapse in fire, the higher stiffness of the floor is required at midspan (where a hinge

Table 1
Collapse Types for Different Scenarios

UB	533 × 210 × 92	406 × 178 × 74	356 × 171 × 51	305 × 165 × 46	305 × 127 × 37
UC	<i>3 Floor fire</i>				
356 × 406 × 235	Strong floor	Strong floor	Strong floor	Strong floor	Weak floor
356 × 368 × 153	Strong floor	Strong floor	Strong floor	Strong floor	Weak floor
305 × 305 × 158	Strong floor	Strong floor	Strong floor	Strong floor	Weak floor
UC	<i>4 floor fire</i>				
356 × 406 × 235	Strong floor	Strong floor	Strong floor	Weak floor	Weak floor
356 × 368 × 153	Strong floor	Strong floor	Strong floor	Weak floor	Weak floor
305 × 305 × 158	Strong floor	Strong floor	Strong floor	Weak floor	Weak floor
UC	<i>5 floor fire</i>				
356 × 406 × 235	Strong floor	Strong floor	Weak floor	Weak floor	Weak floor
356 × 368 × 153	Strong floor	Strong floor	Strong floor	Weak floor	Weak floor
305 × 305 × 158	Strong floor	Strong floor	Strong floor	Weak floor	Weak floor

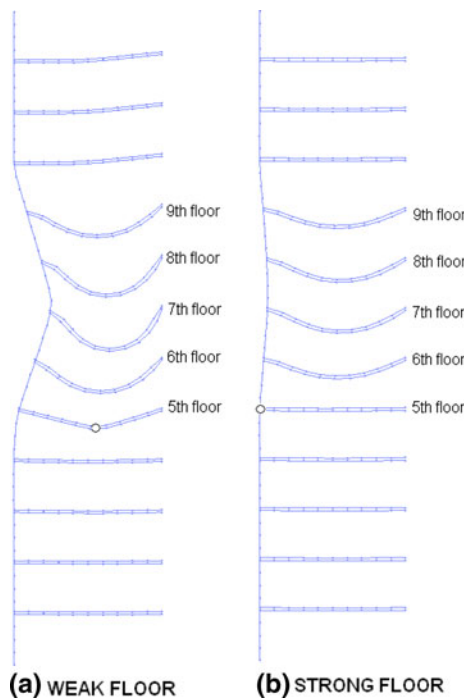


Figure 24. Deformed shapes for a four floor fire (6-9).

should be avoided). In earthquake engineering the relevant floor stiffness relative to the column is that at the ends where a hinge may be allowed to be formed instead of in the column to ensure ductile behaviour.

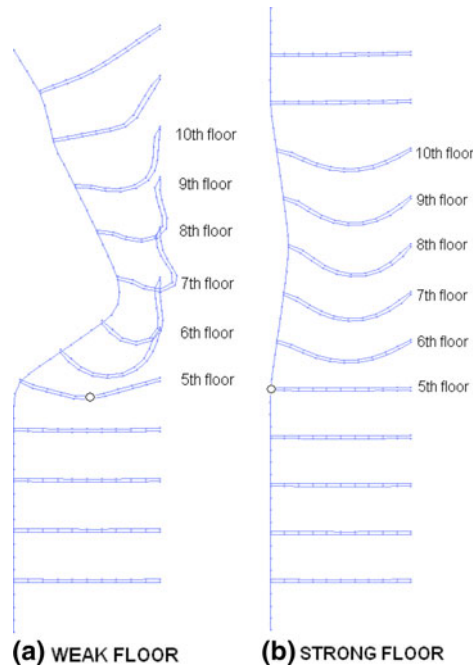


Figure 25. Deformed shapes for a five floor fire (6–10).

The results of the parametric studies performed illustrate that the most probable type of failure is the strong floor collapse. The weak floor collapse has been seen to occur under certain cases too. For the three and four floors fire scenarios the weak floor failure occurred for beams that were outside the serviceability limit state criterion ($\text{span}/300$), but for the five floor scenario the serviceability limit state was satisfied. However, it should be noted that for the three and four fire floor scenarios, the possibility of weak floor collapse should be checked as variable bending stiffness or length along the floors or imperfections could produce different results. More research is required to investigate these mechanisms on other structural forms especially very long span floors made using trusses or cellular beams.

5. Discussion and Conclusions

The analysis presented in this paper has examined the response of the WTC towers in fire and explored various collapse scenarios indicated from previous work. The column “pull in” that triggers the instability of the structure and leads to collapse has been explained. The global behaviour of the structure as well as the local behaviour of the truss has been examined.

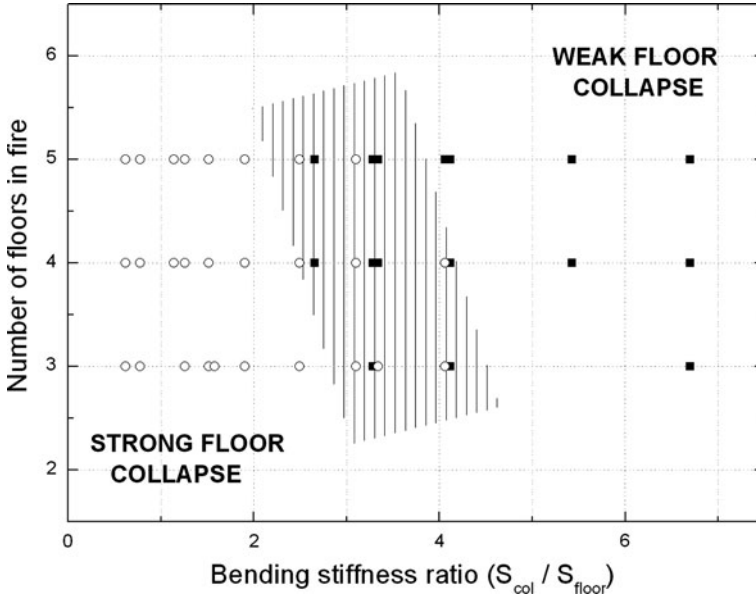


Figure 26. Collapse type envelope for different ratios.

In order to understand tall building collapse in fire, a simpler and more typical steel frame composite structure was modelled. The two different types of collapse mechanisms, weak floor and strong floor failure, have been confirmed and clear distinctions have been drawn in terms their initiation at specific locations in the structure.

Parametric studies were performed in order to evaluate the conditions at which one or the other type of collapse occurs. This has led to a very practical design and assessment criterion of column-floor stiffness ratio against the number of floors on fire. The results of these studies have also shown that the most common type of collapse mechanism is the strong floor collapse, however weak floor collapse becomes more likely with more floors on fire. The knowledge of these mechanisms is of practical use if stakeholders wish to extend the tenability of a tall building structure in a major fire.

Finally, this work also showed the capability of OpenSees to perform progressive collapse analysis under fire since the same global collapse mechanisms seen in previous work [10, 13, 21] have been reproduced without any significant difference. A primary reason for OpenSees being advantageous for this parametric study compared to ABAQUS is that it is more computationally efficient. Its computational efficiency arises primary from its well-written object-oriented architecture and relatively low overhead compared to commercial codes. It would however be easy to perform the same kind of analysis with commercial codes as well. Differences were only seen in failure times after the pulling-in process was

initiated for the generic tall buildings but these resulted from the time scaling that was used in previous research (from 3,600 s to 3.6 s) that underestimated the dynamic effects [21].

Acknowledgements

Authors are grateful to Professor Jose Torero for helpful comments and advice on the draft of this paper and also acknowledge the assistance provided by the Open-Sees team at PEER, UC Berkeley.

References

1. Torero JL (2011) Challenging attitudes on codes and safety. *CTBUH J* 2011(3):36–37
2. Lamster M (2011) Castles in the air. *Sci Am* (special issue) doi:[10.1038/scientificamerican0911-76](https://doi.org/10.1038/scientificamerican0911-76).
3. FEMA (2002) World Trade Center Building performance study: data collection, preliminary observations and recommendations. Technical Report 403. Washington, DC
4. Sunder SS, Gann RG, Grosshandler WL et al (2006) Federal building and fire safety investigation of the World Trade Center disaster: final report of the national construction safety team on the collapses of the World Trade Center towers. NIST, Gaithersburg1
5. (2012) Summary of the structural design of the WTC buildings. *Fire Technol* (WTC special issue, in press)
6. (2012) Summary NIST findings on aircraft damage. *Fire Technol* (WTC special issue, in press)
7. Summary of NIST findings on fire dynamics in WTC 1&2 “*Fire Technology 2012, WTC special issue* (in press)
8. (2012) Summary of NIST findings on fire damage on WTC 1,2 &7”) plus. *Fire Technol* (WTC special issue, in press)
9. Quintiere JG, diMarzo M, Becker R (2002) A suggested cause of the fire-induced collapse of the World Trade Towers. *Fire Saf J* 37(7):707–716. doi:[10.1016/S0379-7112\(02\)00034-6](https://doi.org/10.1016/S0379-7112(02)00034-6)
10. Usmani AS, Chung YC, Torero JL (2003) How did the WTC towers collapse? A new theory. *Fire Saf J* 38(6):501–591. doi:[10.1016/S0379-7112\(03\)00069-9](https://doi.org/10.1016/S0379-7112(03)00069-9)
11. Kodur (2003) Role of fire resistance issues in the collapse of the Twin Towers. In: *Proceedings of the CIB-CTBUH conference on tall buildings, 20–23 October, Kuala Lumpur, Malaysia*
12. Usmani AS (2005) Stability of the World Trade Center Twin Towers structural frame in multiple floor fires. *J Eng Mech* 131(6):654–657. doi:[10.1061/\(ASCE\)0733-9399\(2005\)131:6\(654\)](https://doi.org/10.1061/(ASCE)0733-9399(2005)131:6(654))
13. Flint G, Usmani A, Lamont S, Lane B, Torero J (2007) Structural response of tall buildings to multiple floor fires. *J Struct Eng* 133(12):1719–1732. doi:[10.1061/\(ASCE\)0733-9445\(2007\)133:12\(1719\)](https://doi.org/10.1061/(ASCE)0733-9445(2007)133:12(1719))
14. Baum HR (2005) Simulating fire effects on complex building structures. *Fire Saf Sci* 8:3–18. doi:[10.3801/IAFSS.FSS.8-3](https://doi.org/10.3801/IAFSS.FSS.8-3)
15. Ali F, O’Connor D (2001) Structural performance of rotationally restrained steel columns in fire. *Fire Saf J* 36(7):679–691. doi:[10.1016/S0379-7112\(01\)00017-0](https://doi.org/10.1016/S0379-7112(01)00017-0)

16. Franssen JM (2000) Failure temperature of a system comprising a restrained column submitted to fire. *Fire Saf J* 34:191–207. doi:[10.1016/S0379-7112\(99\)00047-8](https://doi.org/10.1016/S0379-7112(99)00047-8)
17. Huang ZF, Tan KH, Ting SK (2006) Heating rate and boundary restraint effects on fire resistance of steel columns with creep. *Eng Struct* 28(6):805–817. doi:[10.1016/j.engstruct.2005.10.009](https://doi.org/10.1016/j.engstruct.2005.10.009)
18. Shepherd PG, Burgess IW (2011) On the buckling of axially restrained steel columns in fire. *Eng Struct* 33(10):2832–2838. doi:[10.1016/j.engstruct.2011.06.007](https://doi.org/10.1016/j.engstruct.2011.06.007)
19. Quiel ES, Garlock MEM (2010) Parameters for modeling a high-rise steel building frame subject to fire. *J Struct Fire Eng* 1(2):115–134. doi:[10.1260/2040-2317.1.2.115](https://doi.org/10.1260/2040-2317.1.2.115)
20. Torero JL (2011) Forensic analysis of fire induced structural failure: the world trade centre, New York. *ICE J Forensic Eng* 164(2):69–77
21. Usmani A, Roben C, Al-Remal A (2009) A very simple method for assessing tall building safety in major fires. *Int J Steel Struct* 9(1):1–15
22. Weingardt R (2005) Engineering legends. *Am Soc Civil Eng* . doi:[10.1061/\(ASCE\)1532-6748\(2001\)1:1\(58\)](https://doi.org/10.1061/(ASCE)1532-6748(2001)1:1(58))
23. (2011) Opensees Software, University of California, Berkeley, <http://opensees.berkeley.edu/index.php>. Accessed 11 September 2011
24. McKenna FT (1997) Object-oriented finite element programming: frameworks for analysis. Algorithms and parallel computing. Dissertation, University of California, Berkeley
25. Usmani A, Zhang J, Jiang J, Jiang Y, Kotsovinos P, May I, Zhang J (2010) Using OpenSees for structures in fire. In: Proceedings of international conference on structures in fire, 2–4 June, Michigan, USA
26. Neuenhofer A, Filippou FC (1998) Geometrically nonlinear flexibility-based frame finite element. *J Struct Eng ASCE* 124:704–711. doi:[10.1061/\(ASCE\)0733-9445\(1998\)124:6\(704\)](https://doi.org/10.1061/(ASCE)0733-9445(1998)124:6(704))
27. M de Souza R (2000) Force-based finite element for large displacement inelastic analysis of frames. Dissertation, University of California, Berkeley
28. Spacone E, Ciampi V, Filippou FC (1996) Mixed formulation of nonlinear beam finite element. *Comput Struct* 58:71–83. doi:[10.1016/0045-7949\(95\)00103-N](https://doi.org/10.1016/0045-7949(95)00103-N)
29. Spacone E, El-Tawil S (2004) Nonlinear analysis of steel concrete composite structures: state of the art. *J Struct Eng* 130(2):159–168. doi:[10.1061/\(ASCE\)0733-9445\(2004\)130:2\(159\)](https://doi.org/10.1061/(ASCE)0733-9445(2004)130:2(159))
30. Hilber HM, Hughes TJR, Taylor RL (1977) Improved numerical dissipation for time integration algorithms in structural dynamics. *Earthq Eng Struct Dyn* 5:283–292. doi:[10.1002/eqe.4290050306](https://doi.org/10.1002/eqe.4290050306)